Materials Science in Semiconductor Processing 35 (2015) 81–89

Contents lists available at ScienceDirect

Materials Science in Semiconductor Processing

journal homepage: www.elsevier.com/locate/mssp

Effects of time exposure and low power sonochemical treatment on ZnO mesostructures

B.C. Costa [a,*], C. Morilla-Santos [b], P.N. Lisboa-Filho [c]

[a] Universidade Estadual Paulista "Júlio de Mesquita Filho" – UNESP, Programa de Pós-Graduação em Ciência e Tecnologia de Materiais, POSMAT, Bauru, SP, Brazil
[b] Universidade Federal do Ceará – UFC, Departamento de Física, Fortaleza, CE, Brazil
[c] Universidade Estadual Paulista "Júlio de Mesquita Filho" – UNESP, Departamento de Física, Bauru, SP, Brazil

ARTICLE INFO

Available online 19 March 2015

Keywords:
Zinc oxide
Flower-like structures
Sonochemistry

ABSTRACT

A variety of technological applications related to oxide semiconductor-based devices has attracted great interest in the scientific community. Among these materials, zinc oxide (ZnO) has applications in several areas, from light-emitting diodes (LEDs), photovoltaic devices in solar cells and biomaterials. Furthermore, the possibility of application in technological devices highly depends on the synthesis routes employed. Within this context, we investigate the structural and morphological conformation of ZnO structures obtained by low power sonochemical treatment and the effects of time exposure on these mesostructures. To analyze such influences, two samples were prepared without sonochemical treatment with differences in the initial heat-treatment and gas-flux conditions. Another group of six samples was prepared with different time exposures (5, 15, 30, 60, 90 and 120 min) in a low power sonochemical treatment. All the prepared samples were characterized by the XRD associated to Rietveld refinement and SEM. The obtained results analyses indicated that sonochemical treatment was not a necessary condition to obtain highly ordered mesostructures, however, differences in time exposure led to structural and morphological modifications in the ZnO structures. Furthermore, it was observed that the use of vacuum assisted-thermal treatments promotes undesired second phase removal.

1. Introduction

The variety of technological applications related to the development of oxide semiconductor-based devices has attracted great interest in the scientific community, significantly increasing studies related to these materials in the last decades. Among these materials, zinc oxide (ZnO) in particular, has been the object of study of several groups around the world, mainly due to its characteristics of high electronic mobility, high thermal conductivity, wide and direct band gap (3.37 eV at room temperature), large exciton binding energy (60 meV), high chemical stability and recognized antibacterial activity, among others. Such properties make this oxide suitable for a wide range of applications, including its application in transparent thin film transistors, photodetectors, light emitting diodes, laser diodes, gas sensors, varistors, transducers, solar cells, compact cold cathodes, drug carriers, biosensing, treatment and cancer diagnosis, orthopedic coatings and dental implants, among many others [1–8].

It is well known that the properties and, consequently, the applications of a given material fundamentally depend on the applied synthesis routes for its obtainment. Among the chemical routes most commonly employed for the

* Corresponding author.

http://dx.doi.org/10.1016/j.mssp.2015.02.058
1369-8001/

obtainment of ZnO, we can mainly highlight the hydrothermal and sol–gel methods [9,10]. Within this context, solution based chemical routes have attracted great interest, since they provide simple and fast improvements under ambient conditions for semiconductor growth with controlled morphology.

The sonochemical method consists of a chemical and ultrasound association. It is a technique that allows for the preparation of a large variety of nanostructured materials, wherein the chemical effects arise from a phenomenon called acoustic cavitation, which can be understood as a process that consists of the formation, growth and implosive collapse of bubbles in a liquid. In this technique, the formed bubbles have a lifetime of microseconds and transient temperatures of 5000 °C and pressures of 1000 atm in located points have been reported, some of these being the characteristics that lead to high energy chemical reactions [11]. This technique is controlled by parameters including amplitude and frequency of applied sound field, temperature, vapor pressure, density of nuclei in solution, and probe emitting radiation geometry [12].

Furthermore, acoustic cavitation acts as a way to concentrate the diffused ultrasound energy to a single set of conditions, providing materials with unique properties from their precursors dissolved in solution [11]. Regarding the ZnO obtained by the sonochemical method, Jung et al. [13] reported the possibility of morphology control since some of the parameters are controlled, such as precursor concentrations and types, and the power and time of ultrasonic irradiation. These authors reported on the achievement of structures with the following morphologies: nanocups, nanodisks, nanorods, nanospheres and nanoflowers.

In addition to providing different morphologies for ZnO, such as ellipsoidal nanoparticles [14], porous nanospheres [15] octahedral nanoparticles [16], besides the previously mentioned structures, sonochemical treatment can also promote morphological and structural modifications in ZnO nanostructures, as already verified in previous studies from our group, wherein ZnO nanoparticles exhibited the emergence of an amorphous shell around themselves after an ultrasonic treatment using a high ultrasonic irradiation power [17,18].

In the present work, we present an analysis related to time exposure of ultrasonic treatment influences on the morphological and structural characteristics of ZnO mesostructures obtained from a sonochemical method using a low irradiation power of ultrasonic waves.

2. Experimental

Aiming to investigate the effects of time exposure of a low power ultrasonic irradiation on the structural and morphological characteristics, six samples were synthesized with the sonochemical method at different times of sonication (t=5, 15, 30, 60, 90 and 120 min). Furthermore, two samples were prepared without ultrasonic irradiation (t=0 samples).

In the present work, t=0 samples were obtained from solutions wherein 4 g of zinc nitrate hexahydrate ($Zn(NO_3)\cdot 6H_2O$ P.A. – Vetec) was dissolved in 300 ml of deionized water. The pH of the solution was then adjusted to 10, with the addition of 9 ml of ammonium hydroxide. This increase in pH value is required since it allows for the formation of Zn^{2+} and OH^- ions in solution, and consequently, the formation of ZnO. The solutions were then left to rest in order to obtain the precipitate. After this period, the pH value observed was approximately 7. The precipitates were then collected and washed five times in isopropyl alcohol and five times in deionized water using a centrifugal Hermle Labortechnik model Z-326, in 15 min cycles at 12,000 rpm. Lastly, the samples were dried in two distinct processes, one was dried in a muffle furnace and air atmosphere at 80 °C for 24 h (ZnO_t-0_80air) and the other was dried in a vacuum oven at 100 °C for 2 h (ZnO_t-0_100vac).

The same solution mentioned above for synthesis of t=0 samples was used for the samples obtained with different time exposures to sonochemical treatment. Six equal solutions were prepared and submitted to sonochemical treatment for 5, 15, 30, 60, 90 and 120 min in a Sonics VCX-750 ultrasonic processor (20 kHz and 750 W) using an amplitude of 40% and an effective power of 25 W. After this treatment, these solutions were left to rest. All samples were washed as previously mentioned and then dried under the same conditions used for the sample without sonochemical treatment and dried in vacuum and named as ZnO_t-5, ZnO_t-15, ZnO_t-30, ZnO_t-60, ZnO_t-90 and ZnO_t-120, respectively, according to the time exposure to the sonochemical treatment time.

In addition, after the analysis of crystallographic data of all samples obtained from the procedure mentioned above, it was realized a blank test, considering this is an important part of sonochemical reactions, since there is a temperature increasing during these reactions. This test was realized in the temperature of optimum time (60 min) of sonochemical reaction (50 °C), taking account that this temperature is related to the exposure time that resulting in better quality sample (higher crystallinity sample). For the blank test, the same initial solution for the synthesis of all samples mentioned above was used. This solution was kept at 50 °C for 60 min. After this time, the heating was turned off and the solution was then left to rest in order to obtain the precipitate, which was washed as all the previous samples and dried in vacuum at 100 °C for 2 h. The obtained sample from the blank test was named ZnO_Blank and the possible morphological changes were checked.

The identification of the crystalline phases of the samples synthesized as described above was performed by X-ray Diffraction using a RIGAKU D/MAX 2100 PC diffractometer. In addition, the Rietveld refinements were done with GSAS [19] and the interface of EXPGUI [20]. Furthermore, morphological analyses were carried out by Scanning Electron Microscopy using a JEOL microscope model 7500F with theoretical resolution of 1 nm Table 1.

3. Results and discussion

Fig. 1 shows the powder diffraction patterns for the samples. According to this figure, it is possible to note that, except for the ZnO_t-0_80air and ZnO_t-0_100vac

Table 1
Sample labels, sonication times and drying conditions (air/vacuum).

Name	Sonication time (min)	Drying process
ZnO_t-0_80air	0	80 °C/24 h/air
ZnO_t-0_100vac	0	100°/2 h/vacuum
ZnO_Blank	0	100°/2 h/vacuum
ZnO_t-5	5	100°/2 h/vacuum
ZnO_t-15	15	100°/2 h/vacuum
ZnO_t-30	30	100°/2 h/vacuum
ZnO_t-60	60	100°/2 h/vacuum
ZnO_t-90	90	100°/2 h/vacuum
ZnO_t-120	120	100°/2 h/vacuum

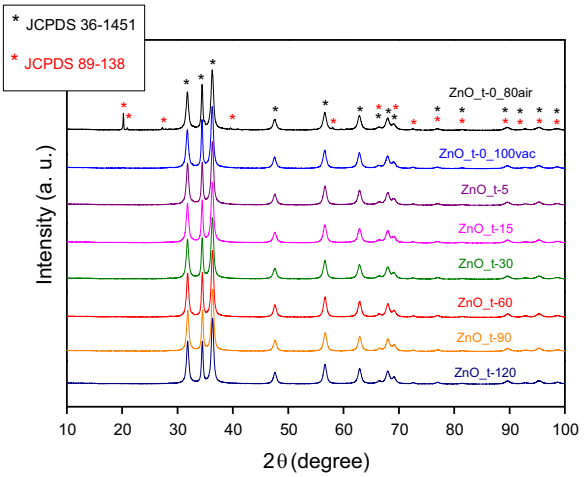

Fig. 1. Powder diffraction patterns of the synthesized samples.

samples, all other samples, including ZnO_Blank sample, were shown to be single phase, with peaks indexed by the ZnO hexagonal phase (Wurtzite - JCPDS 36-1451). The not-single phase samples presented both the ZnO hexagonal phase as well as the $Zn(OH)_2$ phase, wherein the last presents an orthorhombic structure (JCPDS 89-0138).

Rietveld refinements confirmed the presence of zinc hydroxide, as can be seen in Fig. 2(a) and (b). Furthermore, quantitative analyzes for the ZnO_t-0_80air and ZnO_t-0_100vac samples presented values of 3.21 and 1.93 for wt %, respectively, for the $Zn(OH)_2$ phase.

In a previous study, Panda et al. used the sonochemical method to obtain ZnO structures, and they also noted the presence of zinc hydroxide [21]. These authors reported that the initial solution, similar to that used in this current research, was irradiated by ultrasonic waves for 180 min, and after the washing process, the precipitates were dried at 100 °C for 2 h in air atmosphere. Thus, the presence of a larger amount of zinc hydroxide is assumed to be present in the ZnO_t-0_80air sample compared to the ZnO_t-0_100vac sample, and the absence in the other samples is related to the drying process, wherein the vacuum drying process can contribute to the removal of undesired phases.

An additional analysis of the XRD data was also performed. In Fig. 3, the FWHM (Full Width Half Maximum) behavior can be seen as a function of the sonication time for all samples. In this plot, the sample corresponding to the $t=0$ sample is the ZnO_t-0_100vac. Furthermore, the main peak of higher intensity (plane (101)) for each sample and an error of 2% were considered in this analysis.

It is noteworthy that Fig. 3 shows an important behavior for the peak widths. At the beginning of the ultrasonic treatment, the FWHM evidenced an increasing trend, which is related to a decrease in the sample's crystallinity obtained at 5, 15 and 30 min. After 30 min, a significant reduction in the FWHM values was observed, which maintained approximate constant values between 60 and 120 min of sonication, which is attributed to the increase in crystallinity for samples obtained in this interval, or otherwise, the occurrence of a recrystallization process occurring in $t=60$ min. Thus, it was considered that the time $t=60$ min was the optimum time of sonochemical reaction, due to the production of higher crystallinity sample. In this time, the maximum temperature reached during sonochemical reaction was approximately 50 °C and this temperature was used to the blank test achievement. The test results are discussed below.

A possible recrystallization process for ZnO was also verified by Kale et al. [22]. These authors used the hydrothermal method to obtain flower-like ZnO microstructures, and in the synthesis process, a mixture of deionized water, zinc acetate (as Zn^{2+} precursor) and sodium hydroxide (as OH^- precursor) was used. The process of ZnO formation in aqueous solutions was related by Kale et al. and considered in the current work and follows the reactions below:

$$Zn^{2+} + 2(OH)^- \leftrightarrow Zn(OH)_2 \quad (1)$$

$$Zn(OH)_2 + 2(OH)^- \rightarrow Zn(OH)_4^{2-} \quad (2)$$

$$Zn(OH)_4^{2-} \rightarrow ZnO + H_2O + 2OH^- \quad (3)$$

According to Kale et al., the ZnO microstructures were obtained from the direct decomposition of the soluble precursor $Zn(OH)_4^{2-}$ and the growth process involves the following stages: nucleation, growth, dissolution and recrystallization. Even though the methods of synthesis are different, it is believed that the dissolution and recrystallization processes reported by these authors are very similar to the observed in our research. Since both methods are based on solutions, the argument utilized by Kale and co-authors can be used to understand the growth process for the ZnO mesostructures obtained.

In agreement to this previous argument, the addition of $NH_4OH$and $Zn(NO_3)_2 \cdot 6H_2O$ in deionized water provides the reaction between Zn^{2+} and OH^- ions, forming $Zn(OH)_2$ precipitates. However, excess addition of this hydroxide leads to redissolution of $Zn(OH)_2$, forming a homogeneous solution containing the soluble $Zn(OH)_4^{2-}$ specimen. Thus, with the temperature and pressure increasing at the start of the sonochemical process, the $Zn(OH)_4^{2-}$ ions are decomposed into ZnO nanoparticles, which act as nucleus growth. These nanoparticles are highly unstable and quickly aggregate, minimizing the surface energy, growing from smaller and unstable particles and from the decomposition of the $Zn(OH)_4^{2-}$ species, which are deposited on the surface giving rise to the flower-like structures [22].

Thus, according to the above considerations, it is believed that during the first 30 min of sonication, a dissolution process is predominant, wherein coexist, in equilibrium,

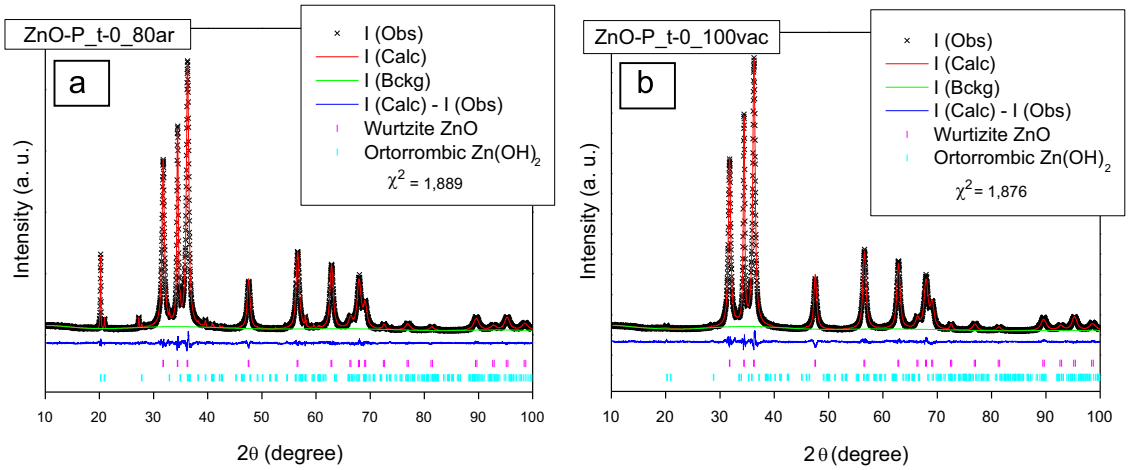

Fig. 2. Rietveld refinements for the (a) ZnO_t-080air and (b) ZnO_t-0_100vac samples.

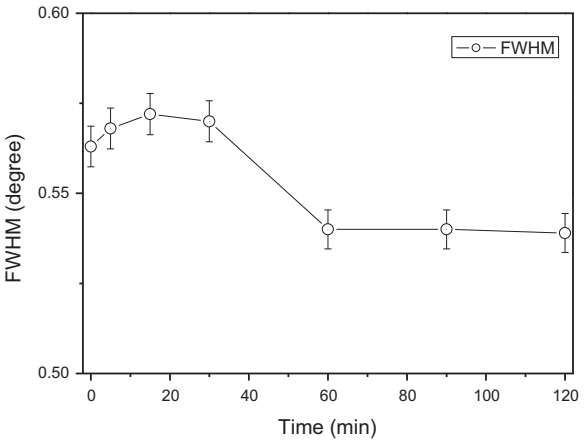

Fig. 3. FWHM in function of the sonication time.

the ZnO nuclei and soluble $Zn(OH)_4^{2-}$ species in the solution. This justifies the decrease in the crystallinity of the samples, verified from the FWHM widening values as shown in Fig. 3 for samples obtained in shorter times (<30 min). After 30 min, the Zn^{2+} with OH^- ions concentration starts to gradually decrease over time, promoting the recrystallization process and allowing the obtainment of higher crystallinity structures. This result can also be observed in Fig. 3, which shows the decrease in the FWHM values for the samples synthesized for 60 min.

Furthermore, Rietveld refinements were also carried out for samples sonochemically treated, which are shown in Fig. 4 (a–f).

Some information can be obtained from these refinements, such as the anisotropic average crystallite size, lattice parameters and the unit cell volume. Fig. 5 shows a plot with the anisotropic average crystallite size (P) as a function of sonication time. In this plot, the sample corresponding to the $t=0$ sample is the ZnO_t-0_100vac. Furthermore, an error of 2% was considered in this analysis.

In Fig. 5, it can be observed that the perpendicular component of average crystallite size (considering a bidimensional crystallite size) was kept practically constant independent of the ultrasonic treatment time. However, the parallel average crystallite size presents a decreasing trend with the start of the sonochemical treatment. In $t=60$ min, and after this time, we observed an increase for these parameter values. Regarding these changes, it is noteworthy that the observed trend in the Fig. 5 plot is very similar to that previously presented in Fig. 3, which refers to the FWHM parameter variation as a function of ultrasonic treatment time for the same samples, wherein we observe the time $t=60$ min as an inflection point for the curve behavior. Thus, the observed behavior related to the average crystallite size analyses reinforce the previously raised hypothesis, that refers to a possible recrystallization process in $t=60$ min.

The obtained values from the Rietveld refinements for the a, b and c lattice parameters and the unit cell volume related to the ZnO hexagonal phase were also analyzed as a function of the sonication time. These data are shown in Fig. 6 (a–c).

The presented data analyses in Fig. 6(b) allow us to observe that the c lattice parameter presents an increase when the ultrasonic treatment starts, followed by a decreasing trend extending until $t=60$ min. After this time, this parameter presents an increasing trend again. With relation to the a and b lattice parameters (Fig. 6(a)) and the unit cell volume (Fig. 6(c)), we can observe a similar behavior, wherein these parameters present a decrease when the ultrasonic treatment starts, followed by an increasing trend that extending until $t=30$ min. In $t=60$ min, both the a and b parameters, as the unity cell volume, presented a minimum value and was immediately followed by an increasing trend. It is noteworthy that regarding the structural parameters, we see a similar behavior in Fig. 3, wherein the time $t=60$ min represents an inflection point and a curve change behavior, which strengthens the hypothesis that a recrystallization process occurs for these samples at this time.

Scanning Electron Microscopy analyses were also performed for all samples. For the $t=0$ samples, the obtained

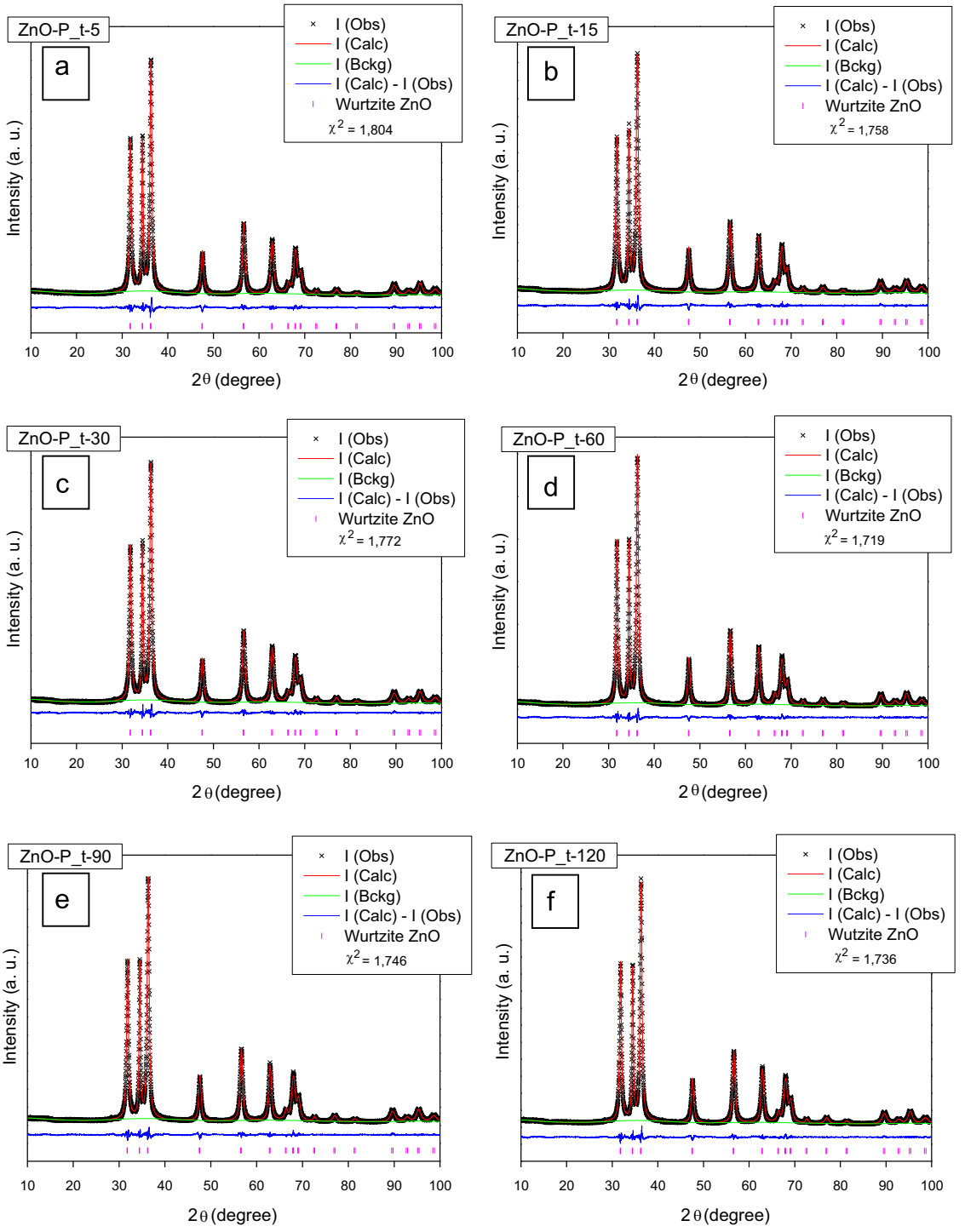

Fig. 4. Structural refinements by the Rietveld method for samples (a) ZnO_t-5; (b) ZnO_t-15; (c) ZnO_t-30; (d) ZnO_t-60; (e) ZnO_t-90; (f) ZnO_t-120.

images are shown in Fig. 7 (a–d), and the images for ZnO_Blank sample are shown in Fig. 7(e–f).

It is possible to observe from Fig. 7 that flower-like structures were obtained for the ZnO_t-0_80air and ZnO_t-0_100vac samples and such structures presented about 2–3 μm as an average size, as well as for ZnO_Blank sample (Fig. 7(e) and (f)). However, significant morphological differences between $t=0$ and ZnO_Blank samples were found. While ZnO_t-0_80air and ZnO_t-0_100vac presented highly rough surfaces, ZnO_Blank sample showed a regular surface. Furthermore, we can observe that the obtained flowers for $t=0$ samples are composed

of smaller rod-like-type substructures with higher regularity, while similar substructures showed higher size for ZnO_Blank sample. Also, for the ZnO_t-0_80air sample, as shown in Fig. 7(a), some particles with regular surfaces are identified, and refers to the $Zn(OH)_2$ second phase, found previously in the XRD analyzes.

In a previous study, Zak et al. [23] also obtained flower-like structures for ZnO prepared by the sonochemical method. It is noteworthy that the synthesis methodology proposed for these authors differs from that employed in this work, wherein we used zinc nitrate hexahydrate as the Zn^{2+} precursor and a pH close to 10 for the sonochemically (or not) treated solutions, while Zak et al. used zinc acetate dihydrate as the Zn^{2+} precursor and not an explicit pH. Furthermore, differently than we observed, 30 min of sonochemical treatment was necessary for these authors to observe flower-like ZnO structures. This result suggests that the zinc nitrate application as the Zn^{2+} precursor favors the obtainment of the flower-like structures, and it is believed that the shaping of these structures is directly influenced by the pH solution to be (or not) sonochemically treated. Furthermore, as reported by Kale et al. [22], the flower-like structures are obtained from the aggregation between smaller particles to minimize the surface energy, thus it is believed that the time of reaction also contributes for these morphology obtainment, since that the precipitation step was longer, allowing the aggregation. Fig. 8 (a–f) presents the SEM images for the ZnO samples obtained from different ultrasonic treatment times.

From Fig. 8 (a–f), we can observe that the obtainment of the flower-like structures was maintained, even after the start of the ultrasonic treatment where similar morphologies evidence a formation independent of time. As described above, we believe that the obtained morphology is related to longer time of reaction that allows the aggregation between

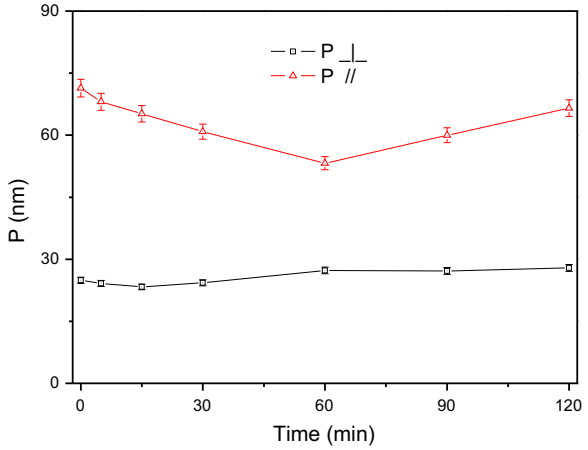

Fig. 5. Anisotropic average crystallite size in function of sonication time.

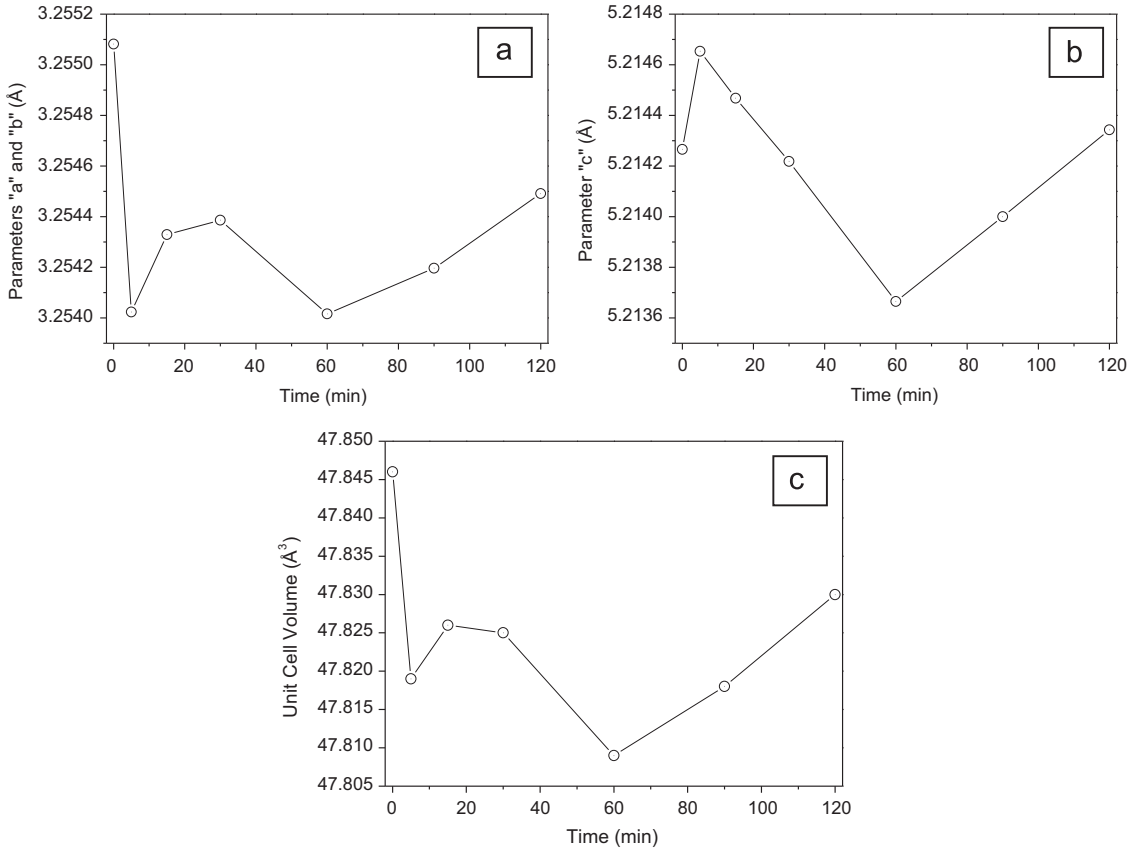

Fig. 6. Parameters obtained from the Rietveld refinements: (a) *a* and *b* lattice parameters; (b) *c* lattice parameter; (c) unit cell volume.

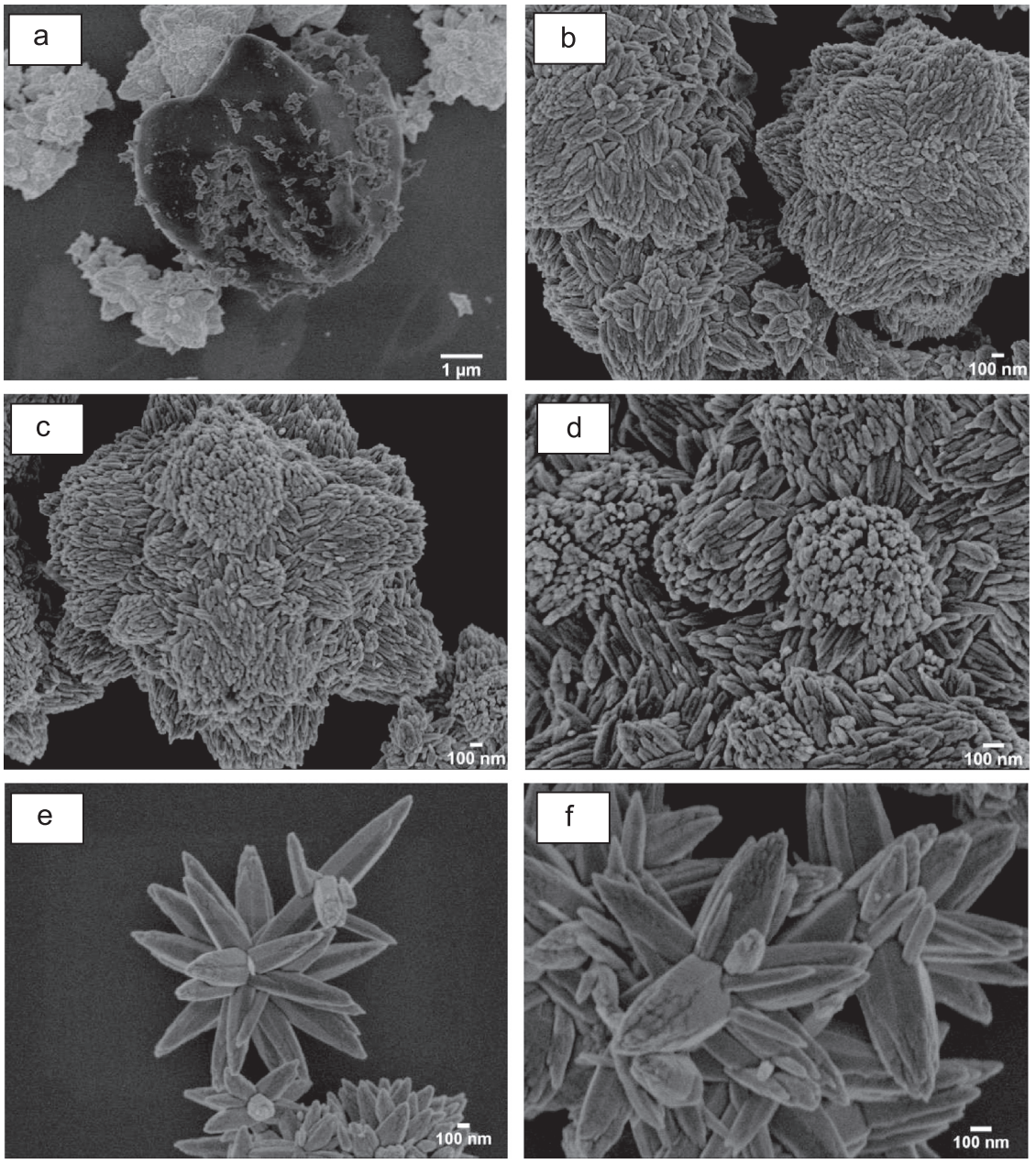

Fig. 7. SEM images for $t=0$ samples and blank test. (a) and (b) ZnO_t-0_80air; (c) and (d) ZnO_*t*-0_100vac; (e) and (f) ZnO_Blank.

the smaller particles, giving rise to the flower-like structures. It is possible to also observe a homogeneous distribution for this morphology type, since no other morphologies were observed for any of the other samples.

A comparative analysis of Figs. 7 and 8 shows that the quality and regularity for the ZnO flower-constituting rods were lost with the ultrasonic treatment, since it was not possible to visualize well-defined rods in the images for the ZnO_t-5, ZnO_t-15 and ZnO_t-30 samples. From the obtained images for these samples, we can note the fragmentation of the rods, forming smaller structures. Such results can be associated to the observed results of the previously presented FWHM analysis, which point to an increasing trend for this parameter until $t=30$ min, besides being related to a decrease of crystallinity in these samples, they are also related to a decrease in the size of the substructures, i.e. rod size decrease, since smaller particles are related to wide diffraction peaks.

A notable FWHM parameter decrease was found in $t=60$ min, keeping approximately constant until $t=120$ min, as previously explained, and is related to an increase in crystallinity for the samples obtained during this time interval. For these samples, from the SEM analyses, it was found that the quality and regularity of flower-constituting

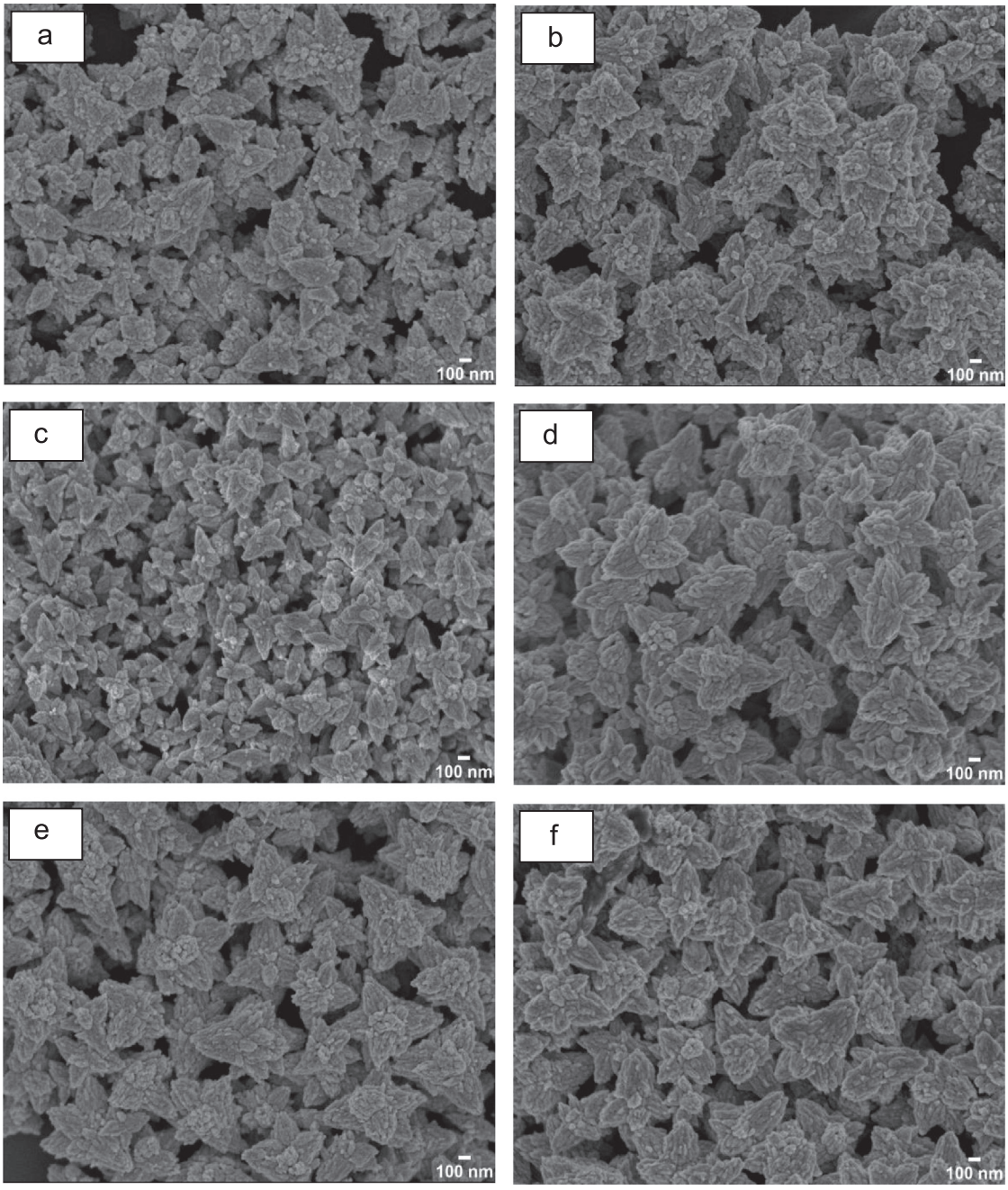

Fig. 8. SEM images for samples obtained from different ultrasonic treatment times: (a) ZnO_t-5; (b) ZnO_t-15; (c) ZnO_t-30; (d) ZnO_t-60; (e) ZnO_t-90; (f) ZnO_t-120.

rods are re-observed and the previously fragmented rods apparently coalesce, increasing in size for the ZnO_t-60, ZnO_t-90 and ZnO_t-120 samples, which is also related to the decrease in FHWM values, as previously presented for these samples, since narrow diffraction peaks are related to larger particles. Thus, the SEM analyzes reinforce the hypothesis established from the XRD analyzes, pointing to a recrystallization process for the ZnO in $t=60$ min.

Another effect observed from the SEM image analyses for samples with different ultrasonic treatment times is the average size decrease for the obtained flower-like structures. While for the flowers referent to the ZnO_*t*-0_100vac and ZnO_Blank samples, the observed particle size was 2–3 μm, an average size distribution of 700–900 nm was found for the flowers referent to the sonochemically treated samples. Furthermore, the sonochemically treated ZnO structures

presented more fragmented morphology if compared to the ZnO_Blank and $t=0$ samples; showing that the ultrasonic treatment presents two effects over these samples: fragmentation and decrease of average particle size.

4. Conclusions

From the results of the obtained analyses, it was possible to conclude that the ultrasonic treatment was not a necessary condition to obtain highly ordered ZnO mesostructures; however, the time exposure presents influences on the structural and morphological characteristics of the ZnO mesostructures obtained, even using low-power irradiation. With regards to the structural characteristics, it was found that the increase in the crystallinity of the samples is a function of the sonochemical treatment time. A recrystallization process in $t=60$ min of time exposure to ultrasonic irradiation was also found. In relation to morphology, it is believed that the obtainment of flower-like structures is related to the use of the zinc nitrate as Zn^{2+} precursor and is directly influenced by the pH of solution and longer time of reaction, including the precipitation step; however the sonochemical treatment does not directly influence on these morphology obtainment, since that flower-like structures were also obtained from the solutions without ultrasonic waves irradiation. It was also observed that the average size of obtained structures was smaller for the ultrasonic irradiated samples in comparison with the non-treated samples. Furthermore, the employed method served as a catalyst for the ZnO precipitate in solution, whereas only the ZnO hexagonal phase was identified for the sonochemically treated samples, while the additional $Zn(OH)_2$ phase was found for the non-treated samples. Moreover, the sonochemical method presents two effects over the obtained structures: fragmentation and decrease of the average particle size. Lastly, the thermal conditions used for the sample drying also presented influences on the undesired second phase removal in the $t=0$ samples since the vacuum dried sample presented a lesser amount of the $Zn(OH)_2$ phase.

Acknowledgments

The authors wish to thank CCDPN-SisNano at Instituto de Química, UNESP – Araraquara, Fundação de Amparo à Pesquisa do Estado de São Paulo – FAPESP (2013/07296-2), Coordenação de Aperfeiçoamento de Pessoal de Nível Superior – CAPES and Conselho Nacional de Desenvolvimento Científico e Tecnológico – CNPq for their financial support.

References

[1] A. Janotti, C.G. Van De Walle, Rep. Prog. Phys. 72 (2009) 126501.
[2] G. Applerot, A. Lipovsky, R. Dror, N. Perkas, Y. Nitzan, R. Lubart, A. Gedanken, Adv. Funct. Mater. 19 (2009) 842–852.
[3] P. Silva-Bermudez, S.E. Rodil, Surf. Coat. Technol. 233 (2013) 147–158.
[4] H. Hong, J. Shi, Y. Yang, Y. Zhang, J.W. Engle, R.J. Nickles, X. Wang, W. Cai, Nano Lett. 11 (2011) 3744–3750.
[5] H. Zhang, B. Chen, H. Jiang, C. Wang, H. Wang, X. Wang, Biomaterials 32 (2011) 1906–1914.
[6] H. Wang, D. Wingett, M.H. Engelhard, K. Feris, K.M. Reddy, P. Turner, J. Layne, C. Hanley, J. Bell, D. Tenne, C. Wang, A. Punnoose, J. Mater. Sci. – Mater. Med. 20 (2009) 11–22.
[7] J. Zhou, N. Xu, Z.L. Wang, Adv. Mater. 18 (2006) 2432–2435.
[8] F. Fang, J. Kennedy, D.A. Carder, J. Futter, P. Murmu, A. Markwitz, J. Nanosci. Nanotechnol. 10 (2010) 8239–8243.
[9] L. Yu, F. Qu, X. Wu, J. Alloy. Compd. 504 (2010) L1–L4.
[10] S. Baruah, J. Dutta, Sci. Technol. Adv. Mater. 10 (2009) 013001.
[11] K.S. Suslick, G.J. Price, Annu. Rev. Mater. Sci. 29 (1999) 295–326.
[12] T.J. Mason, J.P. Lorimer, Sonochemistry: theory, applications and uses of ultrasound in chemistry, Ellis Horwood, Chichester, 1988.
[13] S.H. Jung, E. Oh, K.H. Lee, Y. Yang, C.G. Park, W. Park, S.H. Jeong, Cryst. Growth Des. 8 (2008) 265–269.
[14] X.P. Pu, D.F. Zhang, L.P. Jia, C.H. Su, J. Am. Ceram. Soc. 90 (2007) 4076–4078.
[15] S. Chen, R.V. Kumar, A. Gedanken, A. Zaban, Isr. J. Chem. 41 (2001) 51–54.
[16] C. Pholnak, C. Sirisathitkul, D.J. Harding, J. Phys. Chem. Solids 72 (2011) 817–823.
[17] L.B. Arruda, M.O. Orlandi, P.N. Lisboa-Filho, Ultrason. Sonochem. 20 (2013) 799–804.
[18] B.C. Costa, L.B. Arruda, P.N. Lisboa-Filho, Rev. Fac. Ing. Univ. Antioq. 71 (2014) 9–16.
[19] A.C. Larson, R.B. Von Dreele, Los Alamos National Laboratory Report LAUR 86-748 (2004).
[20] B.H. Toby, J. Appl. Crystallogr. 34 (2001) 210–213.
[21] N.R. Panda, B.S. Acharya, T.B. Singh, R.K. Gartia, J. Lumin. 136 (2013) 369–377.
[22] R.B. Kale, Y.J. Hsu, Y.F. Lin, S.Y. Lu, Superlattices Microstruct. 69 (2014) 239–252.
[23] A.K. Zak, W.H. Majid, H.Z. Wang, R. Yousefi, A.M. Golsheikh, Z.F. Ren, Ultrason. Sonochem. 20 (2013) 395–400.